REPORT No. 741

FLUTTER CALCULATIONS IN THREE DEGREES OF FREEDOM

By THEODORE THEODORSEN and I. E. GARRICK

Langley Memorial Aeronautical Laboratory

LANGLEY FIELD, VA.

NATIONAL ADVISORY COMMITTEE FOR AERONAUTICS

HEADQUARTERS, 1500 NEW HAMPSHIRE AVENUE NW., WASHINGTON, D. C.

Created by act of Congress approved March 3, 1915, for the supervision and direction of the scientific study of the problems of flight (U. S. Code, title 50, sec. 151). Its membership was increased to 15 by act approved March 2, 1929. The members are appointed by the President, and serve as such without compensation.

TECHNICAL COMMITTEES

AERODYNAMICS — **AIRCRAFT MATERIALS** — **INVENTIONS & DESIGNS**
POWER PLANTS FOR AIRCRAFT — **AIRCRAFT STRUCTURES** — **OPERATING PROBLEMS**

Coordination of Research Needs of Military and Civil Aviation

Preparation of Research Programs

Allocation of Problems

Prevention of Duplication

Consideration of Inventions

LANGLEY MEMORIAL AERONAUTICAL LABORATORY

LANGLEY FIELD, VA.

AMES AERONAUTICAL LABORATORY

MOFFETT FIELD, CALIF.

AIRCRAFT ENGINE RESEARCH LABORATORY

CLEVELAND AIRPORT, CLEVELAND, OHIO

Conduct, under unified control, for all agencies, of scientific research on the fundamental problems of flight.

OFFICE OF AERONAUTICAL INTELLIGENCE

WASHINGTON, D. C.

Collection, classification, compilation, and dissemination of scientific and technical information on aeronautics

REPORT No. 741

FLUTTER CALCULATIONS IN THREE DEGREES OF FREEDOM

By THEODORE THEODORSEN and I. E. GARRICK

SUMMARY

The present paper is a continuation of the general study of flutter published in NACA Reports Nos. 496 and 685. The paper is mainly devoted to flutter in three degrees of freedom (bending, torsion, and aileron), for which a number of selected cases have been calculated and presented in graphical form. The results are analyzed and discussed with regard to the effects of structural damping, of fractional-span ailerons, and of mass-balancing. The analysis shows that more emphasis should be put on the effect of structural damping and less on mass-balancing. The conclusion is drawn that a definite minimum amount of structural damping, which is usually found to be present, is essential in the calculations for an adequate description of the flutter case. Theoretical flutter predictions are thus brought into closer agreement with the facts of experience.

A brief discussion is included of a particular biplane that had experienced flutter at about 200 miles per hour. Some simplifications have been achieved in the method of calculation.

INTRODUCTION

Since the publication of the previous flutter papers, the necessity of considering complete cases of three degrees of freedom including the effect of structural damping has become evident. The purpose of the present paper is therefore to present such extensions of general applicability. The calculations herein reported are directly based on methods already given in references 1 and 2. The earlier papers deal, to some extent, with cases of three degrees of freedom and also indicate that the internal structural damping in some cases has a great effect on the flutter velocity; a small value of the internal damping may suffice to bring the flutter velocity from nearly zero to a normal value. Thus, in order to obtain better agreement with practice, the existence of a certain amount of internal damping must be recognized.

A separate investigation on the subject of hysteresis in airplane structures, which has been conducted in the meantime and will be reported in detail elsewhere, shows that a significant amount of internal damping ($g_\alpha > 0.01$) is present, usually with considerable margin. This low value of $g_\alpha \approx 0.01$ is found to be effective in smoothing out the low-velocity flutter values appearing in flutter curves calculated for the case of zero internal damping. A similar effect of different origin is the so-called fractional aileron-span effect. This effect was noted in reference 1 for binary cases and is here also treated for ternary cases. Strangely enough, a reduction in the length of the aileron from that of the full span to a shorter length has a disproportionally large effect on the flutter velocity. Thus, the calculated flutter speed for a full-span aileron may be of a low value; whereas, for a half-span or even a three-quarter-span aileron, it may be nearly normal.

It is of interest to note in connection with the study of three degrees of freedom that the addition of the third degree is the cause of a reduction in the flutter speed based on only two degrees. If a control surface is mass-balanced, is reasonably stiff, and a certain minimum amount of torsional damping is present, the bending-torsion value of the flutter speed will be closely approached.

The following study originated in an investigation of a certain biplane in which flutter had been experienced on a number of occasions. Two of these biplanes were made available at Langley Field for the purpose of the investigation. These biplanes were subjected to the conventional vibration tests in order to obtain the flutter parameters, and the flutter speed was calculated. These calculations were used as the nucleus in the following study of flutter in three degrees of freedom. For readers particularly interested in the biplane mentioned, an appendix (appendix C) has been prepared.

It should further be mentioned that some simplification has been achieved in the method of calculation. This simplification is based on an analogy with Sylvester's method of elimination and reduces quite noticeably the labor of calculating the flutter speed for three degrees of freedom. Appendix B presents a summary of this method.

RESULTS

The results of the flutter calculations are presented in figures 1 to 40. In tables I to IX the constant parameters and the variable parameters are arranged to serve as a key to the figures. In order further to assist the reader in the study of the curves, a brief description of the figures will be given.

It will be noticed that the ordinate for all the curves is the flutter speed in the coefficient form $v/b\omega_\alpha$. The product $b\omega_\alpha$ is thus used as a reference velocity throughout. The symbols used in this paper are defined in appendix A.

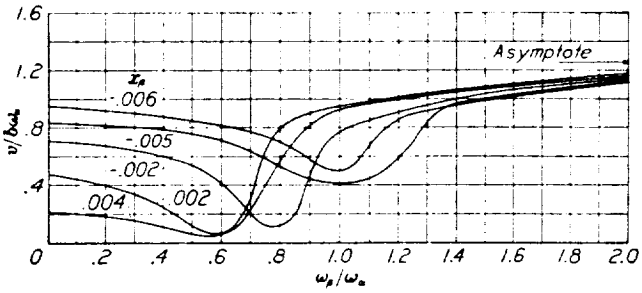

FIGURE 1.—Flutter coefficient $v/b\omega_\alpha$ against frequency ratio $\omega_\beta/\omega_\alpha$ for several values of the aileron unbalance, x_β. x_α,0.2; r_α^2, 1; no damping.

The figures are arranged according to the values of r_α^2: figures 1 to 11, $r_\alpha^2=1$ (biplane case); figures 12 to 28, $r_\alpha^2=0.5$; figures 29 to 36, $r_\alpha^2=0.25$ (monoplane case). Within each group a further arrangement is made according to the value of κ, the wing-density parameter.

Figure 1 shows a number of curves plotted against the aileron frequency ratio $\omega_\beta/\omega_\alpha$, with ω_α thus used as a reference frequency. The wing bending-frequency ratio ω_h/ω_α is kept constant. The curves differ only in the value of x_β, which determines the degree of aileron mass balance. Note the low dips present near $\omega_\beta/\omega_\alpha=1.0$ and the shifting of these low spots with the value of x_β. All the curves approach an asymptote for $\omega_\beta/\omega_\alpha\to\infty$, which corresponds to the bending-torsion binary flutter value.

Figure 2 shows the effect of the torsional structural damping coefficient $g_\alpha=0.01$ on some of the curves of figure 1. Note that the dip in the flutter curves is now eliminated and that the flutter coefficient does not differ by much from its bending-torsion value.

Figure 3 shows the individual effects of the structural damping coefficients g_α, g_β, and g_h on the flutter coefficient for the constant parameters $x_\beta=0.002$ and $\omega_\beta/\omega_\alpha=0.833$. Note that g_α has the greatest effect in increasing the flutter speed.

The parameters for the next set of curves (fig. 4) differ from those of figure 1 only in the value of x_α, which is now 0; that is, the center of gravity of the main wing coincides with the elastic axis at the 40-percent-chord position. Again, for values of x_β of 0 and 0.002, low dips exist near $\omega_\beta/\omega_\alpha=1.0$. For $x_\beta=-0.002$, the low dip does not exist. The bending-torsion flutter value at $\omega_\beta/\omega_\alpha=\infty$ is considerably increased over that for $x_\alpha=0.2$ in figure 1.

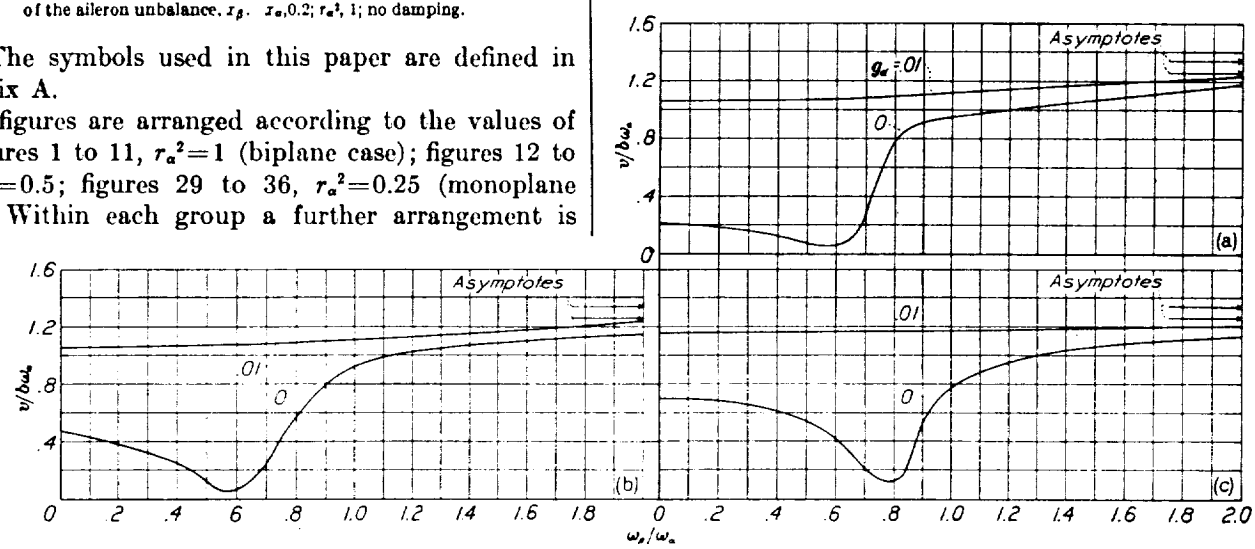

(a) $x_\beta=0.004$.
(b) $x_\beta=0.002$.
(c) $x_\beta=-0.002$.

FIGURE 2.—Flutter coefficient $v/b\omega_\alpha$ against frequency ratio $\omega_\beta/\omega_\alpha$ with and without structural torsional damping. x_α, 0.2; r_α^2, 1.

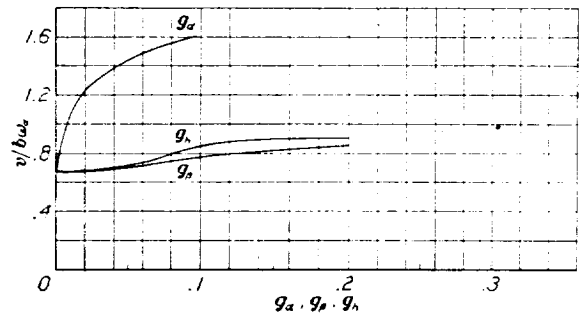

FIGURE 3.—Flutter coefficient $v/b\omega_\alpha$ against structural damping coefficients g_α, g_β, and g_h. $\omega_\beta/\omega_\alpha$, 0.833; x_β, 0.002; r_α^2, 1.

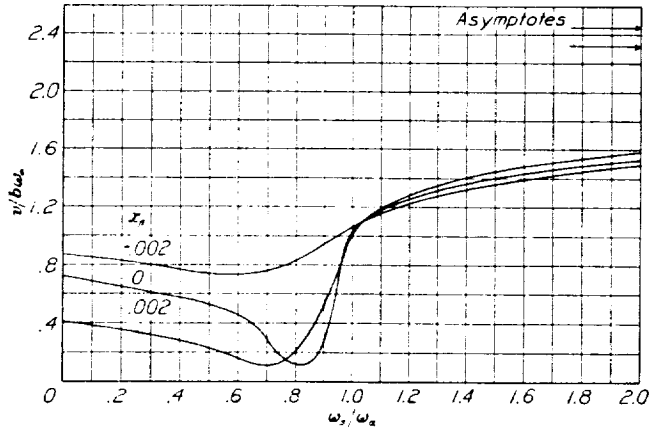

FIGURE 4.—Flutter coefficient $v/b\omega_\alpha$ against frequency ratio $\omega_\beta/\omega_\alpha$ for several values of the aileron unbalance x_β. x_β, 0; r_α^2, 1; no damping.

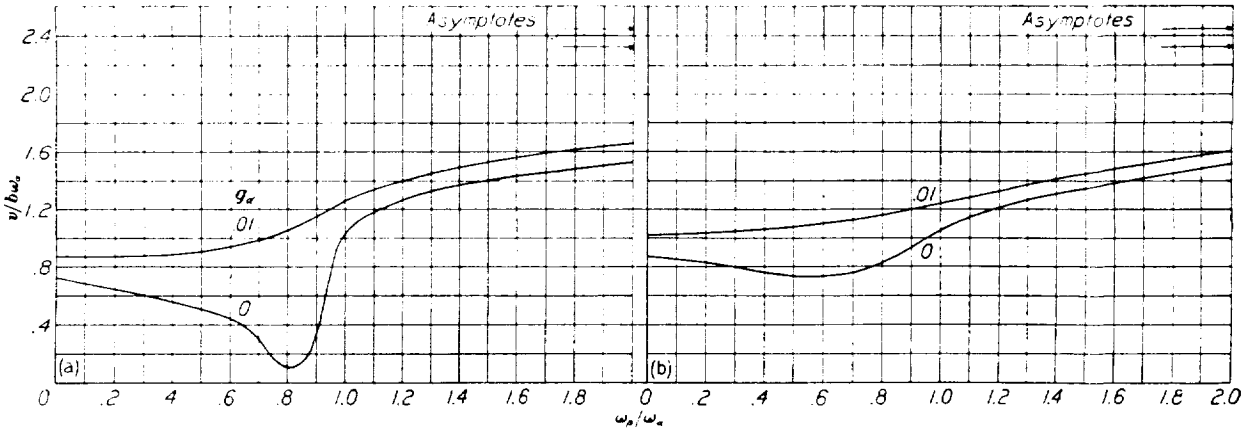

(a) $x_\beta=0$. (b) $x_\beta=-0.002$.

FIGURE 5.—Flutter coefficient $v/b\omega_\alpha$ against frequency ratio $\omega_\beta/\omega_\alpha$, with and without structural torsional damping. x_α, 0; r_α^2, 1.

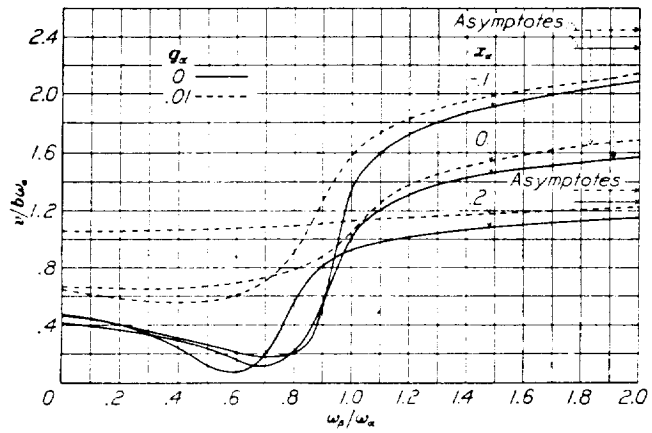

FIGURE 6.—Flutter coefficient $v/b\omega_\alpha$ against frequency ratio $\omega_\beta/\omega_\alpha$ for several values of the wing unbalance x_α, with and without structural torsional damping. x_β, 0.002; r_α^2, 1.

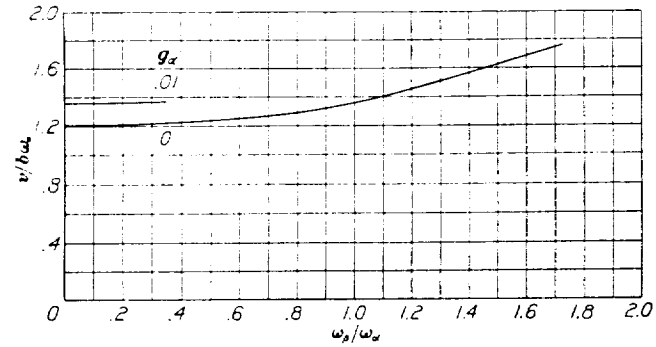

FIGURE 7.—Flutter coefficient $v/b\omega_\alpha$ against frequency ratio $\omega_\beta/\omega_\alpha$ with and without structural torsional damping. x_α, −0.1; x_β, −0.005; r_α^2, 1.

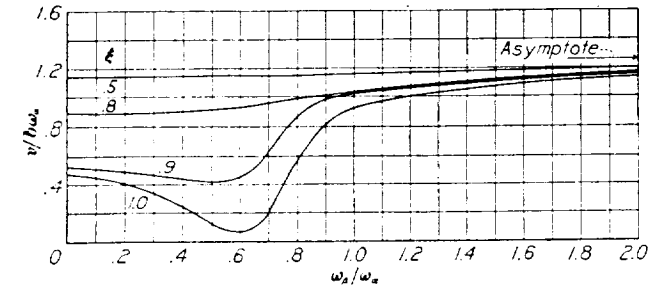

FIGURE 8.—Flutter coefficient $v/b\omega_\alpha$ against frequency ratio $\omega_\beta/\omega_\alpha$ showing the effect of partial-span aileron coefficient ξ. x_β, 0.002; r_α^2, 1.

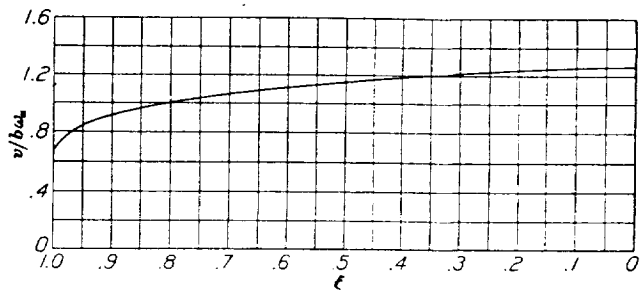

FIGURE 9.—Flutter coefficient $v/b\omega_\alpha$ against partial-span aileron coefficient ξ. $\omega_\beta/\omega_\alpha$, 0.833; r_α^2, 1.

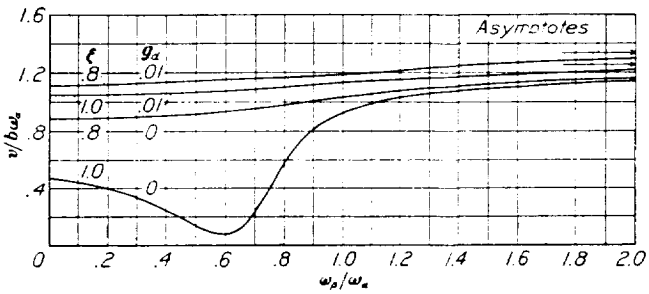

FIGURE 10.—Flutter coefficient $v/b\omega_\alpha$ against frequency ratio $\omega_\beta/\omega_\alpha$ showing the combined effect of structural damping coefficient g_α and partial-span aileron coefficient ξ. x_β, 0.002; r_α^2, 1.

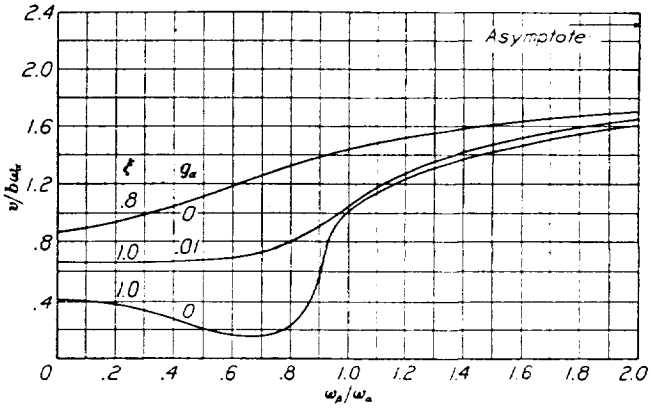

FIGURE 11.—Flutter coefficient $v/b\omega_\alpha$ against frequency ratio $\omega_\beta/\omega_\alpha$ showing the combined effect of the structural damping coefficient g_α and partial-span aileron coefficient ξ. x_β, 0.002; r_α^2, 1.

Figure 5 shows the effect of the torsional structural damping coefficient $g_\alpha=0.01$ in increasing the value of the flutter speed. Figure 6 gives several curves for a

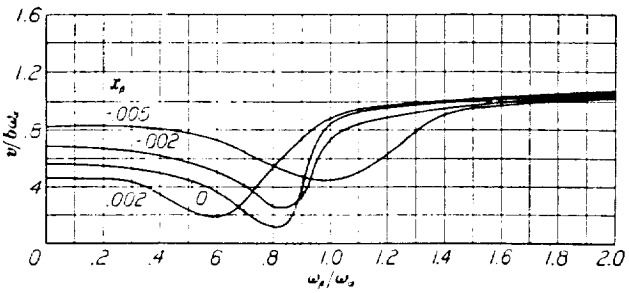

FIGURE 12.—Flutter coefficient $v/b\omega_\alpha$ against frequency ratio $\omega_\beta/\omega_\alpha$ for several values of the aileron unbalance x_β. x_α, 0.2; r_α^2, 0.5; no damping.

curves presented in figure 4 ($x_\alpha=0$, $x_\beta=0.002$). The effect of $g_\alpha=0.01$ is shown for comparison. It is interesting to observe that in the range $\omega_\beta/\omega_\alpha<1.0$ the effect of ξ is significant. In the comparison of this case with figure 10 ($x_\alpha=0.2$), it appears that $\xi=0.8$ is of more influence on the case $x_\alpha=0$ while $g_\alpha=0.01$ is more effective on the case $x_\alpha=0.2$.

The next set of figures (figs. 12 to 28) has been calculated with $r_\alpha^2=0.5$. Figure 12 is similar to figure 1 and shows the flutter-speed coefficient plotted against aileron frequency ratio for several values of x_β. The effect of structural damping is included in figure 13. Figure 14 is a cross plot (similar to fig. 3) against the structural damping coefficients g_α, g_β, and g_h. Figure 15 extends the cases given in figures 13 (a) and 13 (c) to

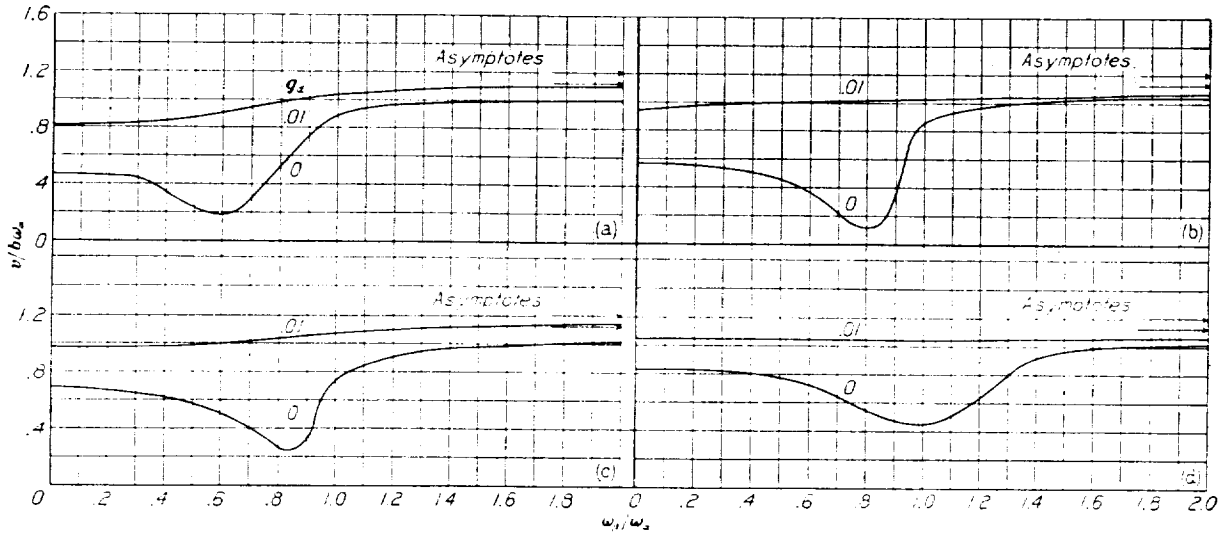

(a) $x_\beta=0.002$. (b) $x_\beta=0$.
(c) $x_\beta=-0.002$. (d) $x_\beta=-0.005$.

FIGURE 13.—Flutter coefficient $v/b\omega_\alpha$ against frequency ratio $\omega_\beta/\omega_\alpha$ with and without structural torsional damping. x_α, 0.2; r_α^2, 0.5; ω_h/ω_α, 0.607.

constant value of x_β of 0.002 and for different values of x_α (0.2, 0, and -0.1), with and without structural damping.

Figure 7 represents a case for which $x_\alpha=-0.1$ and $x_\beta=-0.005$. Case 1 (bending-torsion) is completely stable.

Figure 8 shows the effect of ξ, the partial-span aileron coefficient. The curve $\xi=1.0$ is taken from figure 1 ($x_\beta=0.002$) and is the case of the full-span aileron. Note that even a small reduction to $\xi=0.8$ has a marked favorable effect, especially in the range of frequencies $\omega_\beta/\omega_\alpha<1.0$. As $\xi\to0$ (no aileron), the curves approach the bending-torsion flutter value.

Figure 9 represents a plot against ξ for a constant value of $\omega_\beta/\omega_\alpha$ of 0.833. Figure 10 is intended to show a combined effect of $\xi=0.8$ and $g_\alpha=0.01$. For comparison the separate combinations $\xi=1.0$, $g_\alpha=0$; $\xi=1.0$, $g_\alpha=0.01$; and $\xi=0.8$, $g_\alpha=0$ are also shown.

Figure 11 shows the effect of $\xi=0.8$ on one of the

include other values of the frequency ratio ω_h/ω_α. Figure 16 represents a case of a lighter wing for which κ is 0.25 instead of 0.2. The value of x_β is 0.002; curves with and without structural damping are given. Figure 17 has the same conditions presented in figure 16 except that x_α is equal to 0 instead of 0.2.

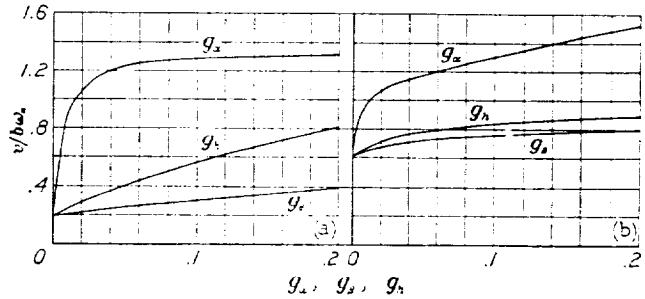

(a) $\omega_\beta/\omega_\alpha$, 0.607. (b) $\omega_\beta/\omega_\alpha$, 0.833.

FIGURE 14.—Flutter coefficient $v/b\omega_\alpha$ against structural damping coefficients g_α, g_β, and g_h. x_β, 0.002; r_α^2, 0.5.

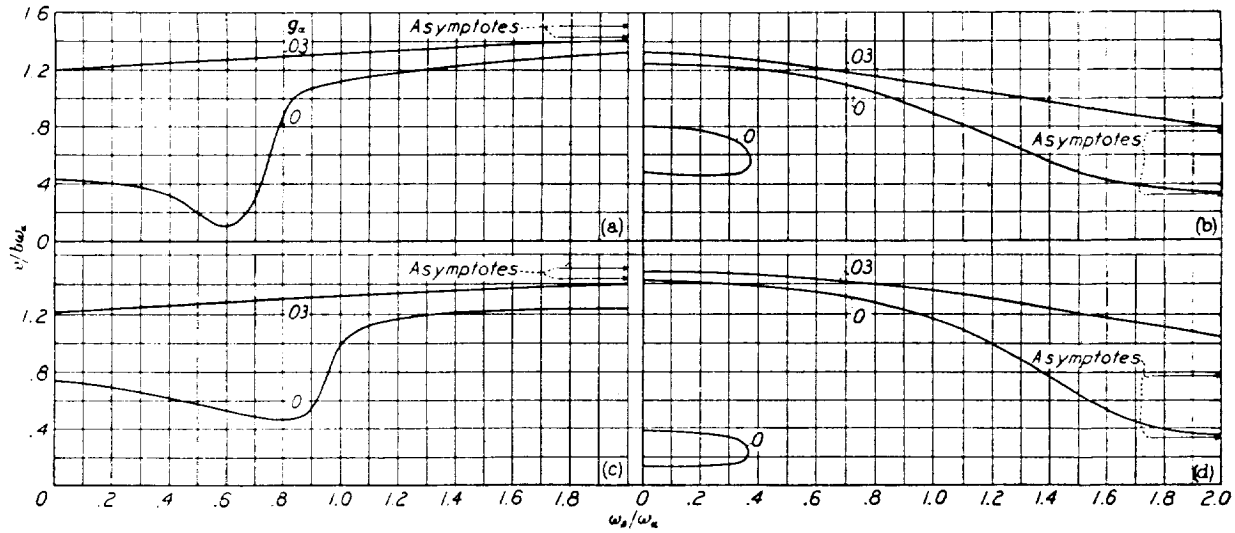

(a) x_β, 0.002; ω_h/ω_α, 0.316.
(b) x_β, 0.002; ω_h/ω_α, 1.0.
(c) x_β, −0.002; ω_h/ω_α, 0.316.
(d) x_β, −0.002; ω_h/ω_α, 1.0.

FIGURE 15.—Flutter coefficient $v/b\omega_\alpha$ against frequency ratio $\omega_\beta/\omega_\alpha$ with and without structural torsional damping. x_α, 0.2; r_α^2, 0.5; (cf. figs. 13 (a) and 13 (c)).

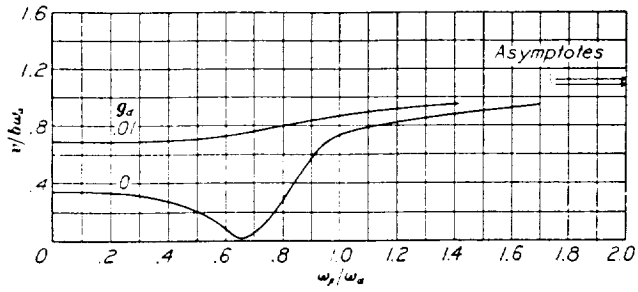

FIGURE 16.—Flutter coefficient $v/b\omega_\alpha$ against frequency ratio $\omega_\beta/\omega_\alpha$ with and without structural torsional damping. x_α, 0.2; x_β, 0.002; κ, 0.25; r_α^2, 0.5.

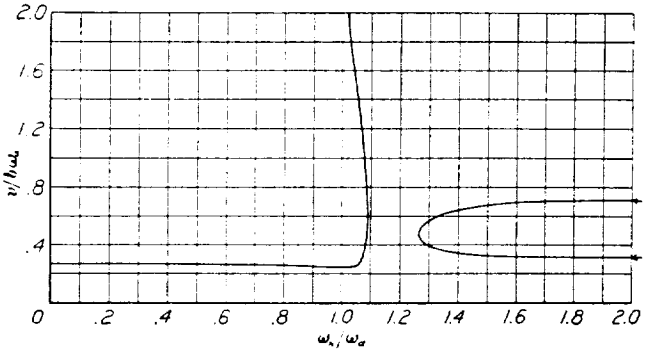

FIGURE 18.—Flutter coefficient $v/b\omega_\alpha$ against wing bending-frequency ratio ω_h/ω_α. $\omega_\beta/\omega_\alpha$, 0.5; x_β, 0.002; κ, 0.25; r_α^2, 0.5; no damping.

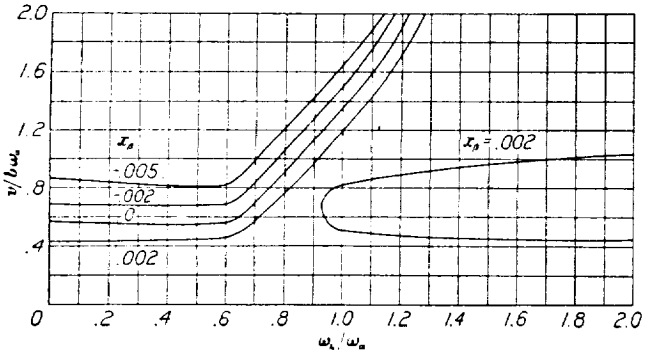

FIGURE 20.—Flutter coefficient $v/b\omega_\alpha$ against wing bending-frequency ratio ω_h/ω_α for several values of the aileron unbalance x_β. $\omega_\beta/\omega_\alpha$, 0; κ, 0.2; r_α^2, 0.5; no damping.

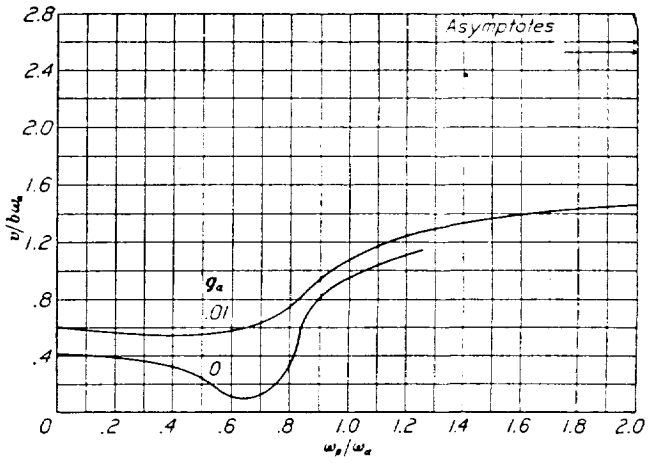

FIGURE 17.—Flutter coefficient $v/b\omega_\alpha$ against frequency ratio $\omega_\beta/\omega_\alpha$ with and without structural torsional damping. x_α, 0; x_β, 0.002; κ, 0.25; r_α^2, 0.5.

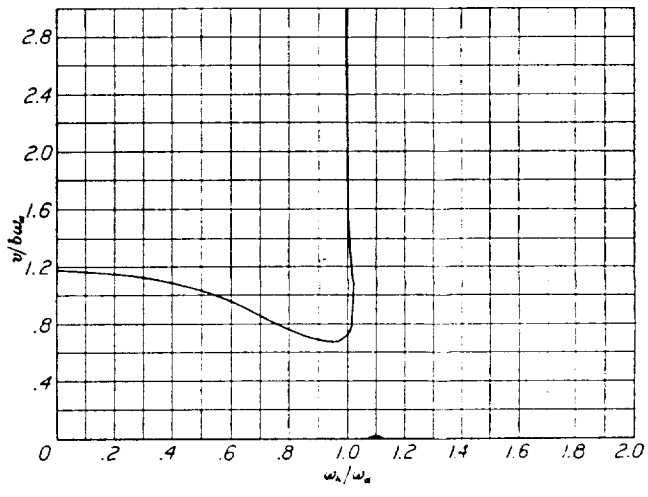

FIGURE 19.—Flutter coefficient $v/b\omega_\alpha$ against wing bending-frequency ratio ω_h/ω_α. $\omega_\beta/\omega_\alpha$, 1.0; x_β, 0.002; κ, 0.25; r_α^2, 0.5; no damping.

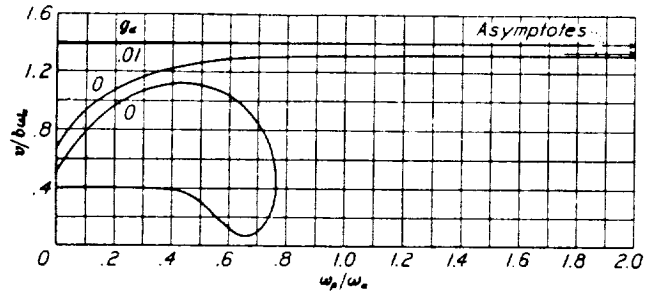

FIGURE 21.—Flutter coefficient $v/b\omega_\alpha$ against frequency ratio $\omega_\beta/\omega_\alpha$ with and without structural torsional damping. x_β, 0.002; κ, 0.125; r_α^2, 0.5; ω_h/ω_α, 0.607.

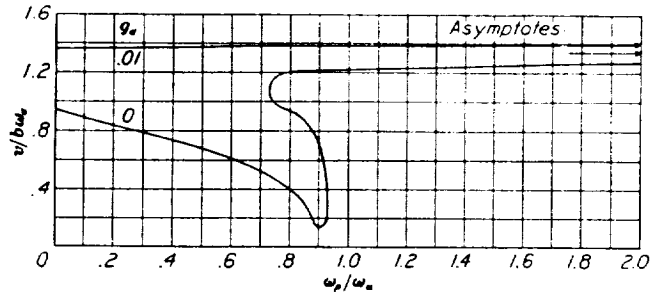

FIGURE 22.—Flutter coefficient $v/b\omega_\alpha$ against frequency ratio $\omega_\beta/\omega_\alpha$ with and without structural torsional damping. x_β, —0.002; κ, 0.125; r_α^2, 0.5; ω_h/ω_α, 0.607.

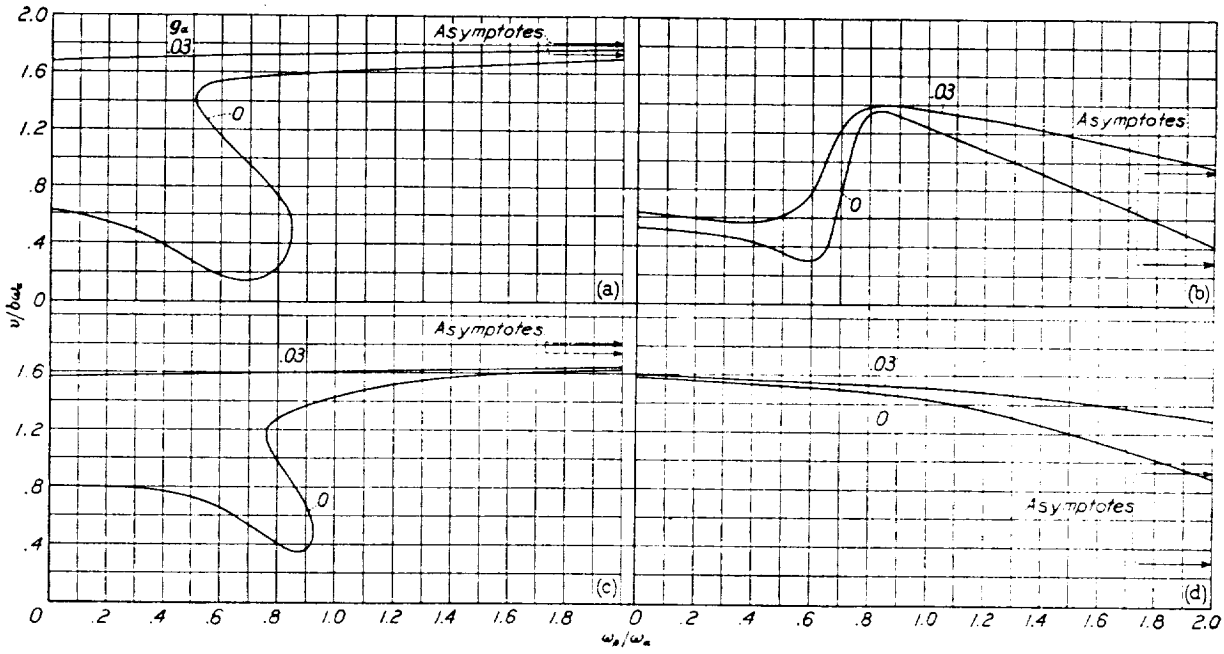

(a) x_β=0.002; ω_h/ω_α=0.316.
(b) x_β=0.002; ω_h/ω_α=1.0.
(c) x_β=−0.002; ω_h/ω_α=0.316.
(d) x_β=−0.002; ω_h/ω_α=1.0.

FIGURE 23.—Flutter coefficient $v/b\omega_\alpha$ against frequency ratio $\omega_\beta/\omega_\alpha$ with and without structural torsional damping. (See also figs. 21 and 22.) κ, 0.125; r_α^2, 0.5.

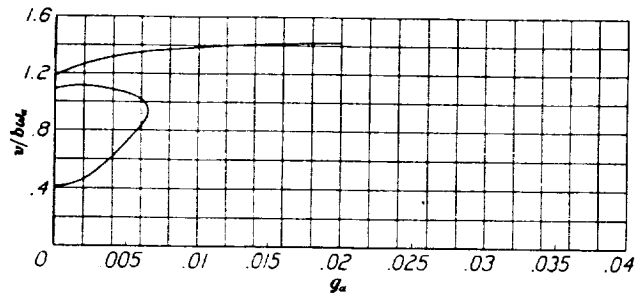

FIGURE 24.—Flutter coefficient $v/b\omega_\alpha$ against structural damping coefficient g_α. $\omega_\beta/\omega_\alpha$, 0.316; x_β, 0.002; κ, 0.125; r_α^2, 0.5.

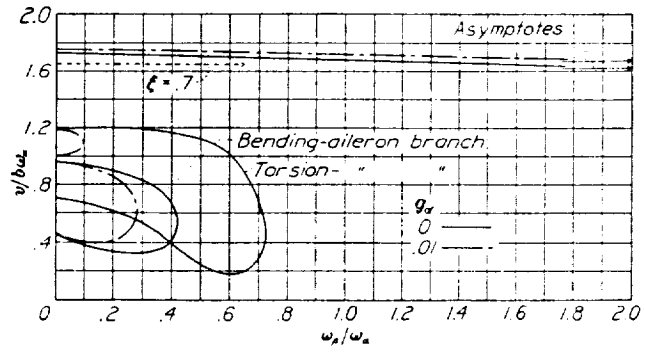

FIGURE 25.—Flutter coefficient $v/b\omega_\alpha$ against frequency ratio $\omega_\beta/\omega_\alpha$ showing the combined effect of the structural damping coefficient g_α and partial-span aileron coefficient ξ. x_β, 0.002; κ, 0.083; r_α^2, 0.5.

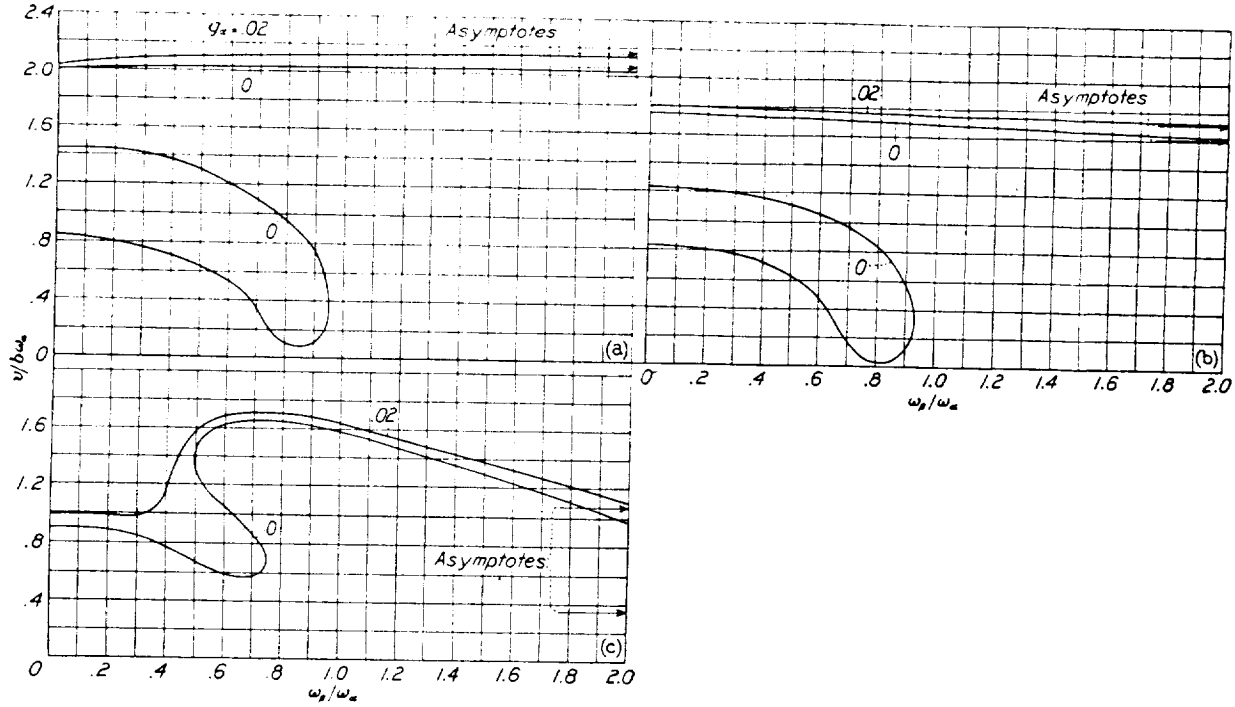

(a) ω_h/ω_α, 0.316.
(b) ω_h/ω_α, 0.607.
(c) ω_h/ω_α, 1.0.

FIGURE 26.—Flutter coefficient $v/b\omega_\alpha$ against frequency ratio $\omega_\beta/\omega_\alpha$ with and without structural torsional damping. x_β, 0; r_α, 0.2; κ, 0.083; r_α^2, 0.5.

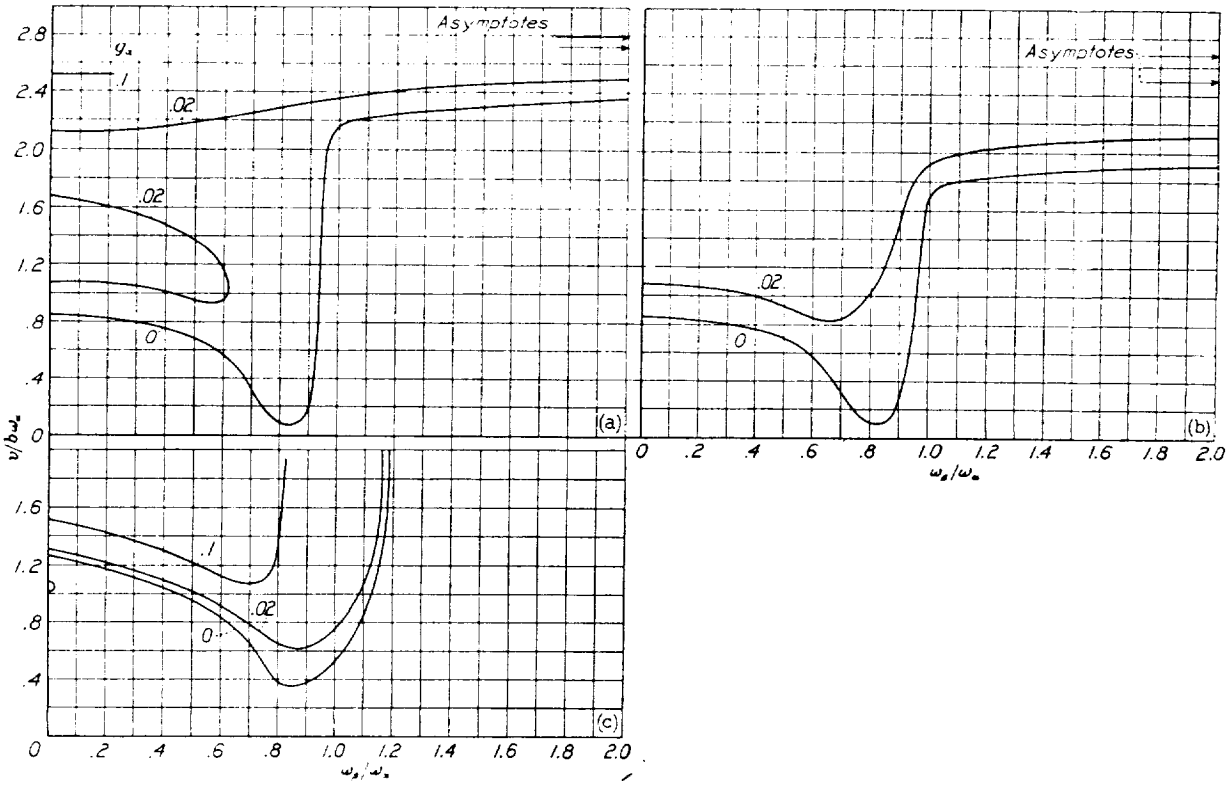

(a) ω_h/ω_α, 0.316.
(b) ω_h/ω_α, 0.607.
(c) ω_h/ω_α, 1.0.

FIGURE 27.—Flutter coefficient $v/b\omega_\alpha$ against frequency ratio $\omega_\beta/\omega_\alpha$ with and without structural torsional damping. x_β, 0; r_α, 0; κ, 0.083; r_α^2, 0.5.

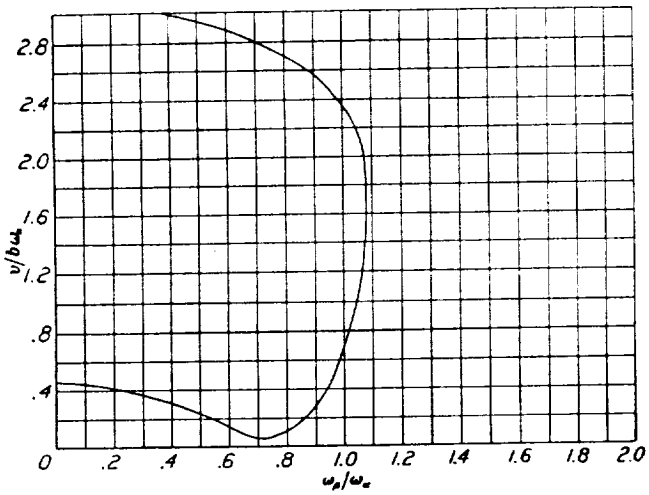

FIGURE 28.—Flutter coefficient $v/b\omega_\alpha$ against frequency ratio $\omega_\beta/\omega_\alpha$. ω_h/ω_α, 1.0; x_α, 0; κ, 0.25; r_α^2, 0.5; no damping.

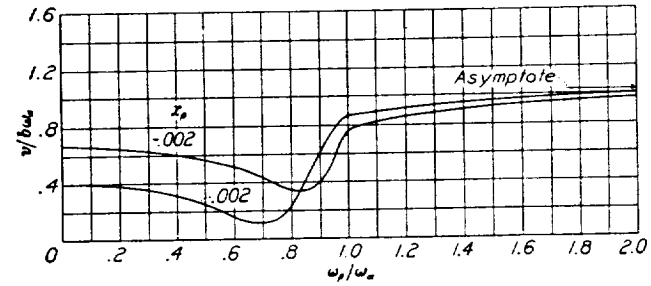

FIGURE 29.—Flutter coefficient $v/b\omega_\alpha$ against frequency ratio $\omega_\beta/\omega_\alpha$ for two values of aileron unbalance x_β. r_α^2, 0.25; no damping.

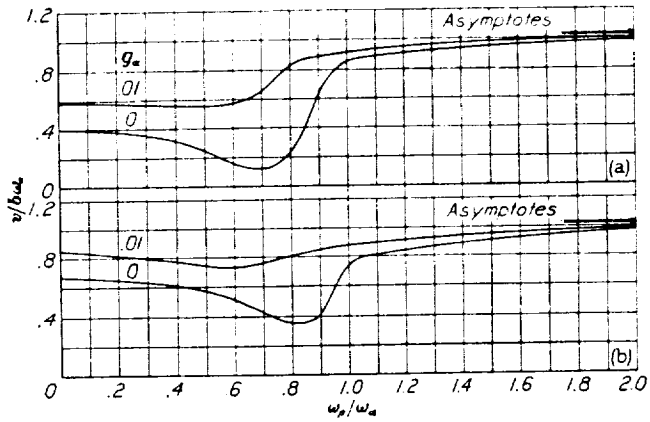

(a) x_β, 0.002. (b) x_β, −0.002.

FIGURE 30.—Flutter coefficient $v/b\omega_\alpha$ against frequency ratio $\omega_\beta/\omega_\alpha$ with and without structural torsional damping. r_α^2, 0.25; ω_h/ω_α, 0.607.

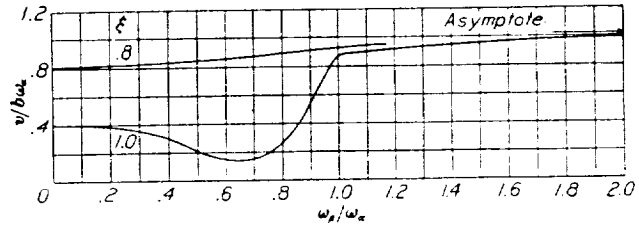

FIGURE 31.—Flutter coefficient $v/b\omega_\alpha$ against frequency ratio $\omega_\beta/\omega_\alpha$ for two values of the partial-span aileron coefficient ξ. x_β, 0.002; r_α^2, 0.25.

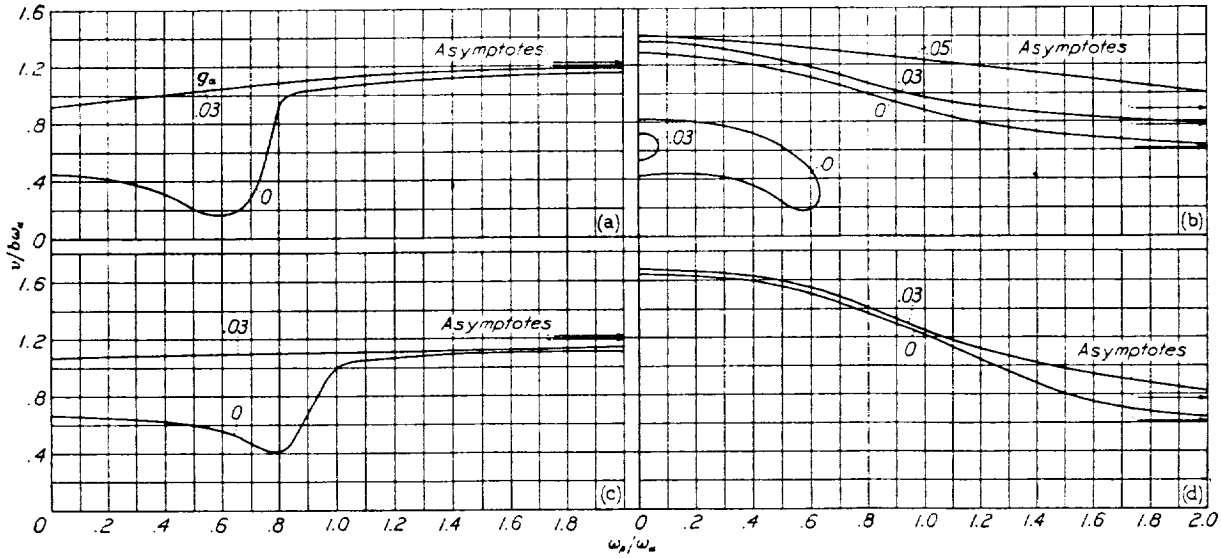

(a) x_β, 0.002; ω_h/ω_α, 0.316. (b) x_β, 0.002; ω_h/ω_α, 1.0.
(c) x_β, −0.002; ω_h/ω_α, 0.316. (d) x_β, −0.002; ω_h/ω_α, 1.0.

FIGURE 32.—Flutter coefficient $v/b\omega_\alpha$ against frequency ratio $\omega_\beta/\omega_\alpha$ with and without structural torsional damping. (See also fig. 30.) κ, 0.2; r_α^2, 0.25.

Figure 18 is a plot of the flutter coefficient against the wing bending-frequency ratio, for a constant value of $\omega_\beta/\omega_\alpha = 0.5$. The case $\omega_h/\omega_\alpha = \infty$ corresponds now to the binary case, torsion-aileron. The branch representing essentially this case is easily evident. Figure 19 differs from figure 18 only in the value of $\omega_\beta/\omega_\alpha$, which is now 1.0. The branch representing torsion-aileron is now gone. (The small singular branch on the axis near $\omega_h/\omega_\alpha = 1.1$ can be shown to disappear completely with a very small amount of friction.)

Figure 20 differs from figure 18 in the value of κ, which is now 0.2, and also in the value of $\omega_\beta/\omega_\alpha$, which is now 0. In addition, several values of x_β have been employed. Note that the aileron-torsion branch beyond $\omega_h/\omega_\alpha=1.0$ exists only for the largest unbalance, $x_\beta=0.002$.

Figure 21 differs from the parallel cases shown by curves $x_\beta=0.002$ in figures 12 and 16 only in the value of κ, which is now 0.125; that is, it represents a heavier wing or a higher altitude. Note that $x_\beta=0.002$ does not eliminate the torsion-aileron branch. The effect of $g_\alpha=0.01$ produces a flutter curve, the ordinate of which is remarkably near the bending-torsion value.

Figure 22 differs from figure 21 in the value of x_β, which is now -0.002. The low dip near $\omega_\beta/\omega_\alpha=1.0$ is eliminated for a value of $g_\alpha=0.01$. Figure 23 extends the cases of figures 21 and 22 to two other values of the frequency ratio ω_h/ω_α.

Figure 24 is a plot of the flutter coefficient against g_α for the constant value of $x_\beta=0.002$ and $\omega_\beta/\omega_\alpha=0.316$. (See fig. 21.) Note that the torsion-aileron branch is gradually eliminated and vanishes for $g_\alpha\approx 0.006$.

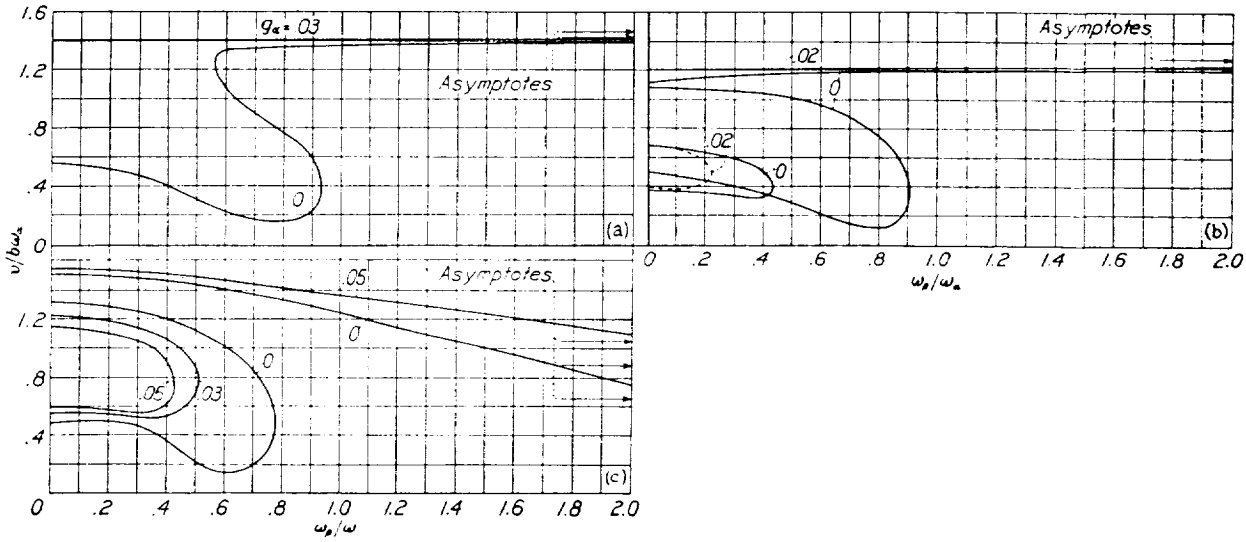

(a) ω_h/ω_α, 0.316.
(b) ω_h/ω_α, 0.607.
(c) ω_h/ω_α, 1.0.

FIGURE 33.—Flutter coefficient $v/b\omega_\alpha$ against frequency ratio $\omega_\beta/\omega_\alpha$ with and without structural torsional damping. κ, 0.125; r_α^2, 0.25; x_β, 0.002.

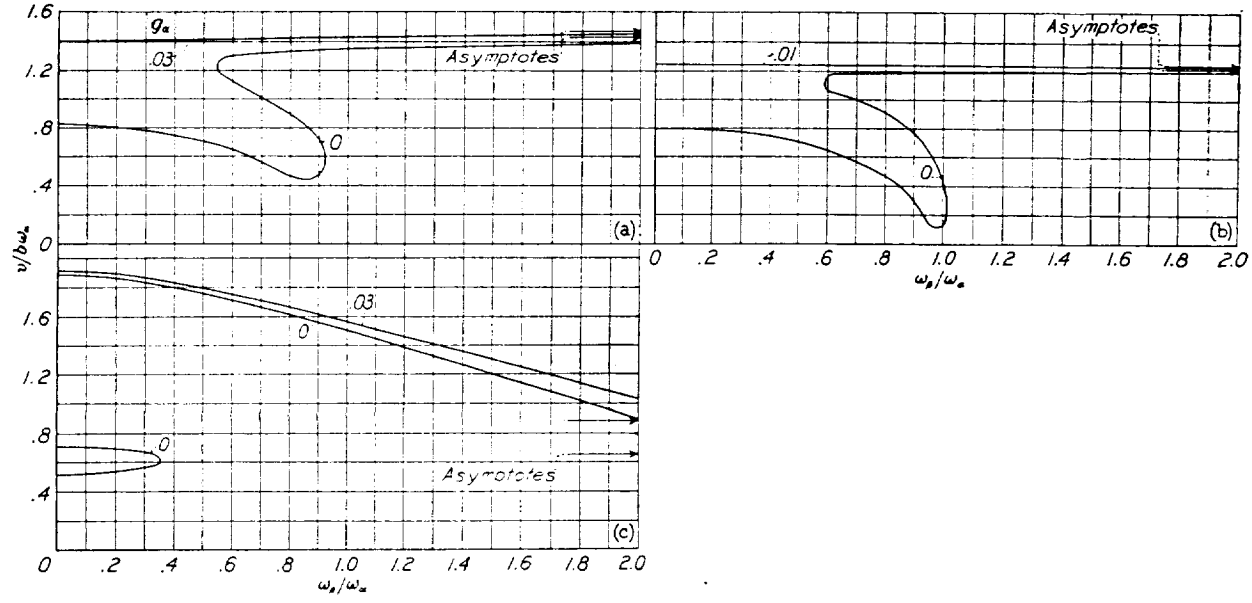

(a) ω_h/ω_α, 0.316.
(b) ω_h/ω_α, 0.607.
(c) ω_h/ω_α, 1.0.

FIGURE 34.—Flutter coefficient $v/b\omega_\alpha$ against frequency ratio $\omega_\beta/\omega_\alpha$ with and without structural torsional damping. κ, 0.125; r_α^2, 0.25; x_β, −0.002.

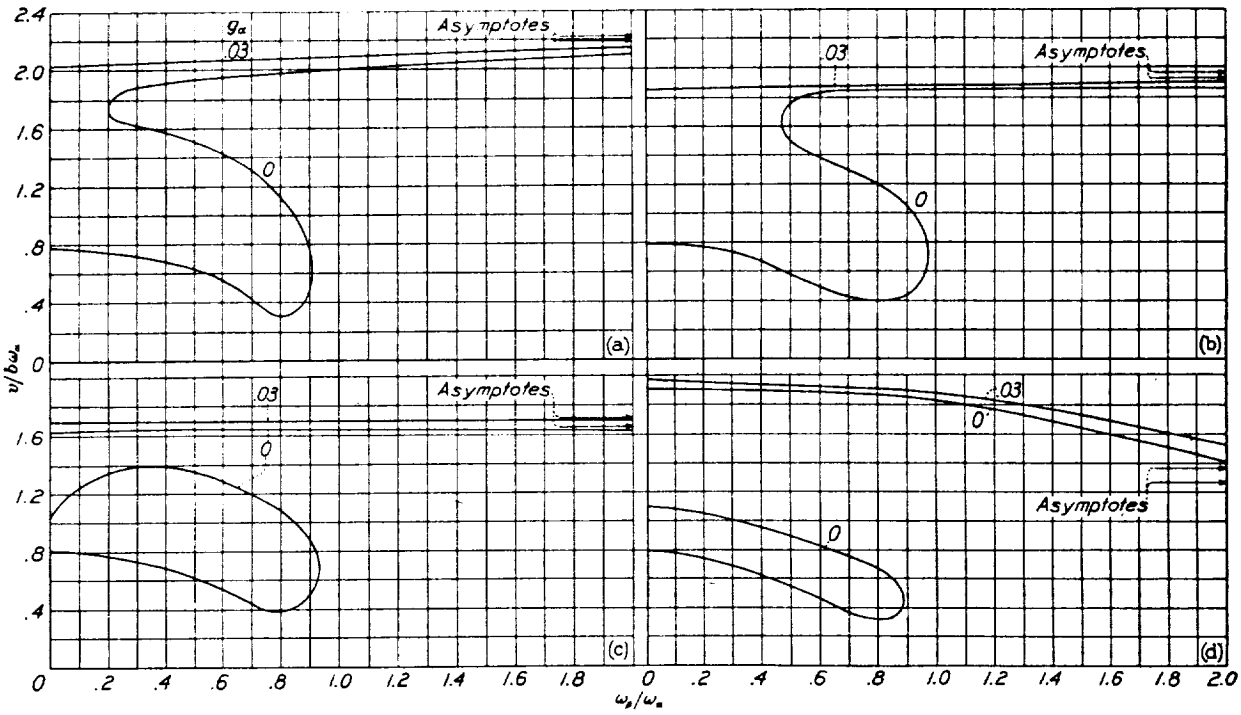

(a) ω_h/ω_α, 0.316.
(b) ω_h/ω_α, 0.5.
(c) ω_h/ω_α, 0.707.
(d) ω_h/ω_α, 1.0.

FIGURE 35.—Flutter coefficient $v/b\omega_\alpha$ against frequency ratio $\omega_\beta/\omega_\alpha$ with and without structural torsional damping. κ, 0.0752; r_α^2, 0.25; x_β,0.

Figure 25 represents a still heavier wing ($\kappa=0.083$). This curve shows that $x_\beta=0.002$ does not eliminate either the torsion-aileron branch or the bending-aileron branch for low values of $\omega_\beta/\omega_\alpha$. The value $\xi=0.7$ as shown eliminates the low branches. The value $g_\alpha=0.02$ eliminates the torsion-aileron branch but has little influence on the bending-aileron branch. Figures 26 and 27 represent similar cases with $x_\beta=0$ and with several values of the frequency ratio ω_h/ω_α. In the cases represented by figure 26 ($x_\alpha=0.2$) the center of gravity of the wing is at 50-percent chord and for those of figure 27 ($x_\alpha=0$) the center of gravity is at 40-percent chord.

Figure 28 represents a case in which $\kappa=0.25$, $x_\alpha=0$, and $\omega_h/\omega_\alpha=1.0$. The figure shows that the bending-torsion flutter branch is eliminated and only the torsion-aileron branch exists. This branch can also be eliminated by increasing the value of g_α.

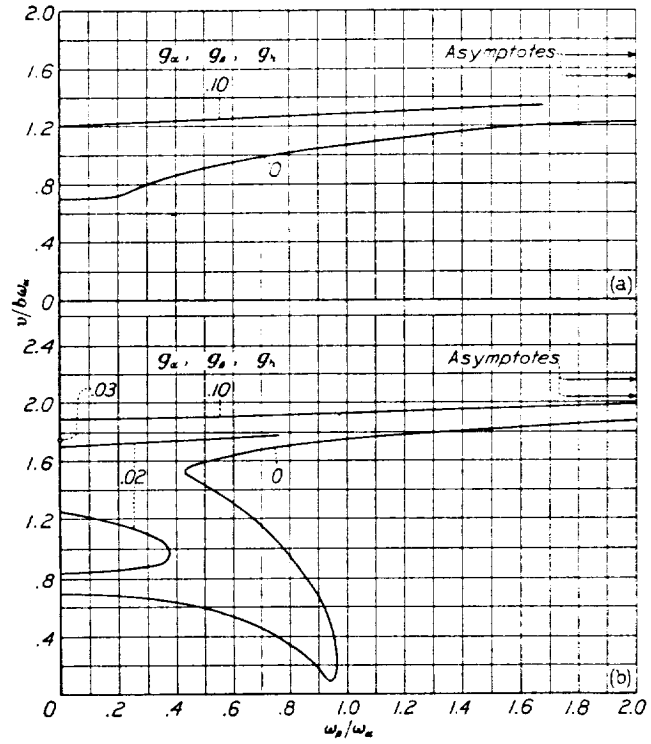

(a) κ, 0.25.
(b) κ, 0.1.

FIGURE 36.—Flutter coefficient $v/b\omega_\alpha$ against frequency ratio $\omega_\beta/\omega_\alpha$. r_α, 0.2; r_α^2, 0.25.

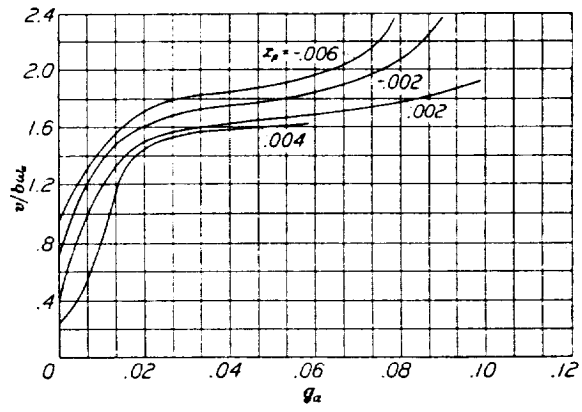

FIGURE 37.—Flutter coefficient $v/b\omega_\alpha$ against the structural damping coefficient g_α in antisymmetrical cases for several values of the aileron unbalance x_β. $\omega_\beta/\omega_\alpha$, 0; ω_h/ω_α, 0.

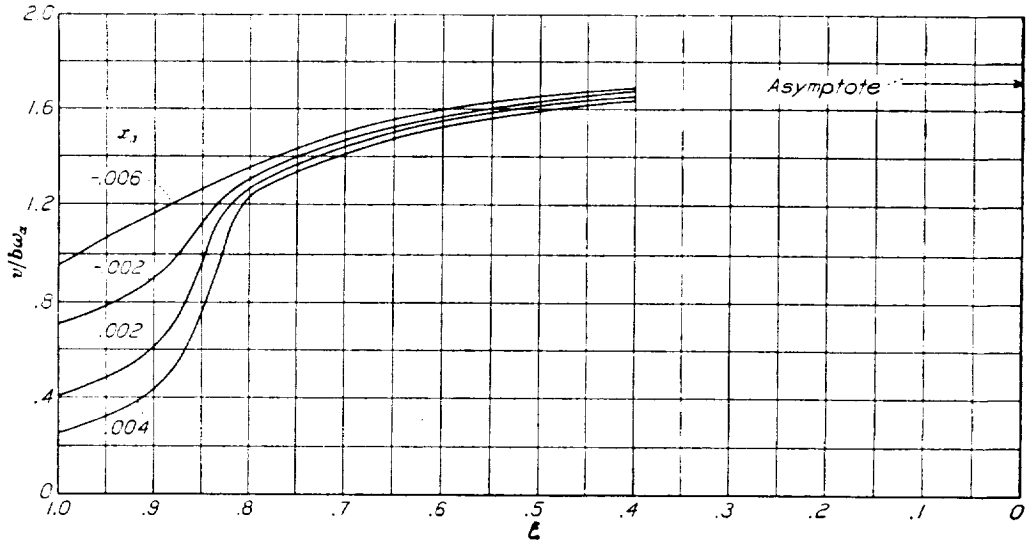

FIGURE 38.—Flutter coefficient $v/b\omega_\alpha$ against partial-span aileron coefficient ξ in the antisymmetrical cases for several values of the aileron unbalance x_β. $\omega_\beta/\omega_\alpha$, 0; ω_h/ω_α, 0.

The next set of figures (figs. 29 to 36) have been calculated with $r_\alpha^2=0.25$ (monoplane case). Figure 29 shows the flutter coefficient plotted against $\omega_\beta/\omega_\alpha$ for two values of x_β: 0.002 and −0.002. The effect of structural damping, $g_\alpha=0.01$, is shown in figure 30 and the effect of the partial-span aileron coefficient ξ is shown in figure 31. Figure 32 extends the cases of figure 30 to other values of the bending-frequency ratio ω_h/ω_α; figures 33 and 34 represent parallel cases for a heavier wing, $\kappa=0.125$.

Figure 35 represents a monoplane case with parameters based on a modern heavy pursuit airplane. For completeness, several curves are shown with different values of the bending-frequency ratio ω_h/ω_α. Figure 36 is based on the parameters for a modern large airplane. Two values of κ are presented: 0.25 and 0.1.

The rest of the figures were calculated for two constant values: $\omega_\beta/\omega_\alpha=0$ and $\omega_h/\omega_\alpha=0$ (antisymmetrical flutter cases). Figure 37 shows the flutter coefficient plotted against g_α for four values of x_β (0.004, 0.002, −0.002, and −0.006). It is observed that the effect of g_α is quite significant. Figure 38 shows the flutter coefficient plotted against ξ for the same values of x_β that were used in figure 37. The effect of ξ in figure 38 is rather large. Figure 39 is a cross plot of figure 38, with x_β as the abscissa. Figure 40 is a plot of the flutter coefficient against g_α for three values of r_α^2 (1, 0.5, and 0.25) and for two values of x_β (0.002 and −0.002).

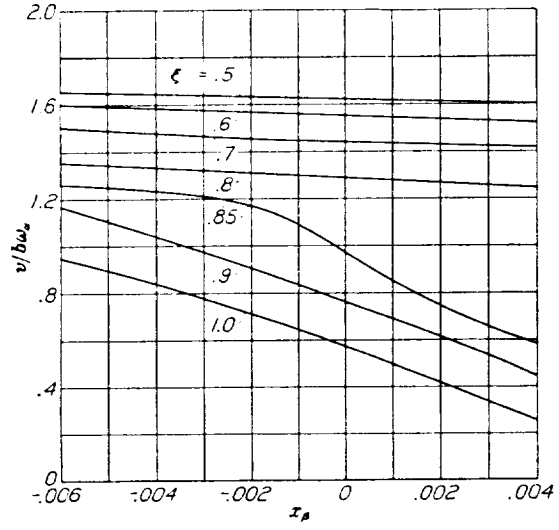

FIGURE 39.—Flutter coefficient $v/b\omega_\alpha$ against aileron unbalance x_β in the antisymmetrical cases for several values of the partial-span aileron coefficient ξ. $\omega_\beta/\omega_\alpha$, 0; ω_h/ω_α, 0.

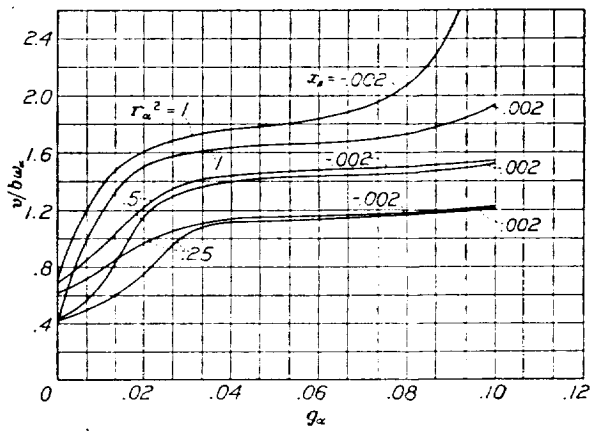

FIGURE 40.—Flutter coefficient $v/b\omega_\alpha$ against the structural damping coefficient g_α in the antisymmetrical cases for three values of r_α^2 and two values of aileron unbalance x_β. $\omega_\beta/\omega_\alpha$, 0; ω_h/ω_α, 0.

DISCUSSION

The first noteworthy observation in the case of three degrees of freedom is the distinct dip in the flutter curve at values of $\omega_\beta/\omega_\alpha$ somewhat less than unity when structural damping is neglected. Apparently the aileron under these circumstances is very nearly in mechanical resonance with the wing in torsion. It is further observed that the flutter velocity remains rather low in this range of values of the aileron frequency. Since the aileron frequency in most practical cases is definitely less than that of the wing torsion, the region below unity is of the most significance.

There are two types of aileron response: One type corresponds to symmetrical wing motion and the other type corresponds to an antisymmetrical motion. The frequency of the first type is of the order of one-half to three-fourths of the torsion frequency and the frequency of the second type is zero. It is noted that the elimination by mass-balancing of flutter resulting from the symmetrical type of response may be difficult, particularly if the aileron frequency is close to the wing-torsion frequency; whereas, the antisymmetrical type is more favorably affected by normal mass-balancing of the aileron. It is also to be noted that the wing damping is unusually effective in removing the dip in the flutter curve. Indeed, for comparatively light structures a value of the torsional damping coefficient g_α of 0.01 brings the flutter velocity almost back to its full bending-torsion value. Significantly, the torsional damping seems to be the most effective. Heavier structures appear to be less susceptible to the effect of damping. In fact, a larger value of g_α is needed and apparently it may be necessary also to provide damping in one or both of the other degrees of freedom (fig. 25).

A partial-span aileron has a rather profound effect on the dip in the flutter curve, which is similar to the effect of the damping. A reduction of the effective aileron length ξ from 1.0 to 0.8 practically restores the normal value of the flutter speed.

It is rather evident from the present study that the effect of mass-balancing has been overemphasized in the earlier literature. Of significance is the fact that a pronounced dip exists in the flutter curve even for an overbalanced aileron (fig. 1). The aileron balancing seems to become most effective for the case in which the wing itself is overbalanced (fig. 7). This case is only of academic interest. Overbalancing alone does not present a solution of the general case of three degrees of freedom; the appropriate value of the flutter speed cannot be obtained solely by any practicable method of balancing.

On the other hand, the greatest beneficial effect of damping is obtained for the unbalanced, that is, the normal wing (fig. 6). Only in this case is the full bending-torsion value nearly reached. In the range of frequencies $\omega_\beta/\omega_\alpha < 1$ the flutter speed of the overbalanced wing remains much lower than that of the normal wing. It is further noted that the beneficial effect of aileron balance is small when a small amount of damping is present (fig. 2).

For the antisymmetrical case with no damping present, $\omega_h=0$, it is observed that the balancing of the aileron is more effective. For a given value of the torsional damping coefficient ($g_\alpha=0.01$) the gain from balancing is not large. The effect of the fractional aileron is very marked. At $\xi=0.8$ the flutter velocity equals the torsion-bending value independently of the balance coefficient.

CONCLUSION

It has been shown that mass-balancing is of less significance than has heretofore been attributed to it. The profound effect of internal structural damping has been shown. For the normal, unbalanced wing a small amount of damping removes the dip in the flutter curve and substantially yields the torsion-bending value of the flutter velocity. The large beneficial effect of the fractional-span aileron has been indicated. These statements apply to light, low-density structures and apply to a lesser degree as the wing density is increased. Because of the complexity of the problem, too general conclusions cannot be safely made and detailed calculations of individual cases are still needed. The included graphs, which cover a fairly representative field, should be of value for specific studies and should furnish numerical solutions in a number of cases.

LANGLEY MEMORIAL AERONAUTICAL LABORATORY,
NATIONAL ADVISORY COMMITTEE FOR AERONAUTICS,
LANGLEY FIELD, VA., *June 7, 1941.*

APPENDIX A

LIST OF NOTATION

α angle of attack (fig. 41)

β aileron angle (fig. 41)

h vertical distance (fig. 41)

b half chord, used as reference unit length

a coordinate of elastic axis (also called axis of rotation or torsional axis) (fig. 41). Location of elastic axis in percentage total chord measured from leading edge is

$$100\,\frac{1+a}{2} \text{ or } a=\frac{2\ (\text{elastic axis})}{100}-1$$

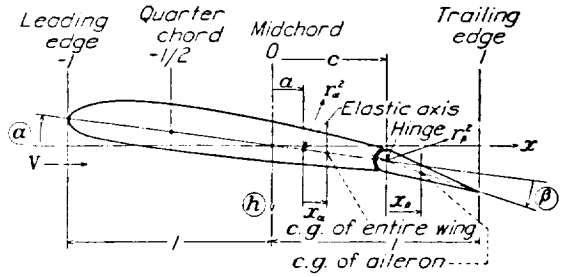

FIGURE 41.—Half chord b is used as the unit length. The positive directions of α, β, and h are indicated by arrows. Note that a is measured from midchord and x_α is measured from the elastic axis positive to the right. Also note that x_β is a "reduced" parameter and not the actual distance from the hinge to the center of gravity of the aileron.

c coordinate of aileron hinge axis (fig. 41). Location of aileron hinge axis in percentage total chord measured from leading edge is

$$100\,\frac{1+c}{2} \text{ or } c=\frac{2\ (\text{aileron hinge})}{100}-1$$

ρ mass of air per unit volume

M mass of wing per unit span length

$\kappa=\frac{\pi\rho b^2}{M}$ ratio of mass of cylinder of air of diameter equal to chord of wing to mass of wing, both taken for equal length along the span; this ratio may be expressed as $\kappa=0.24\ (b^2/W)\ (\rho/\rho_0)$ where W is weight in pounds per foot span, b is in feet, and ρ/ρ_0 is ratio of air density to standard air

$x_\alpha=\frac{S_\alpha}{Mb}$ location of center of gravity of wing-aileron system *measured from a* (fig. 41); S_α, static moment of wing-aileron per unit span length referred to a. Location of center of gravity in percentage total chord measured from the leading edge is

$$100\,\frac{1+a+x_\alpha}{2} \text{ or}$$

$$a+x_\alpha=\frac{2(\text{center of gravity})}{100}-1$$

$x_\beta=\frac{S_\beta}{Mb}$ *reduced* location of center of gravity of aileron referred to c (fig. 41); S_β, static moment of aileron per unit span length referred to c. M refers to total wing mass and not to mass of aileron alone

$r_\alpha=\sqrt{\frac{I_\alpha}{Mb^2}}$ radius of gyration of wing aileron referred to a (fig. 41); I_α, moment of inertia of wing aileron about elastic axis per unit span length

$r_\beta=\sqrt{\frac{I_\beta}{Mb^2}}$ *reduced* radius of gyration of aileron referred to c (fig. 41); I_β, moment of inertia of aileron about c per unit span length

C_α torsional stiffness of wing around a per unit span length

C_β torsional stiffness of aileron around c per unit span length

C_h stiffness of wing in bending per unit span length

$\omega_\alpha=\sqrt{\frac{C_\alpha}{I_\alpha}}$ natural angular frequency of torsional vibrations around a in vacuum ($\omega_\alpha=2\pi f_\alpha$, where f_α is in cycles per sec)

$\omega_\beta=\sqrt{\frac{C_\beta}{I_\beta}}$ natural angular frequency of torsional vibrations of aileron around c

$\omega_h=\sqrt{\frac{C_h}{M}}$ natural angular frequency of wing in bending

t time

v speed of forward motion

ω angular frequency of wing vibrations

$k=\frac{\omega b}{v}$ *reduced* frequency=number of waves in wake in a distance equal to semichord $\times 2\pi$

$1/k$ reduced wave length—length of one wave of wake in terms of a distance equal to semichord $\times 2\pi$

$v/b\omega_\alpha$ flutter-speed coefficient

$g_\alpha,\ g_\beta,\ g_h$ structural damping coefficients; πg corresponds approximately to the usual logarithmic decrement

ξ partial-span aileron coefficient. Note that this coefficient is not the geometric ratio but an "effective" value of the order of $[\int f(\alpha)dz]^2/\int f^2(\alpha)dz$, where the integral in the numerator is taken over the aileron span and that in the denominator is taken over the full span; $f(\alpha)$ represents the spanwise amplitude of (flutter) torsion mode

APPENDIX B

METHOD OF ELIMINATION AS APPLIED TO FLUTTER CALCULATIONS

The treatment of the flutter problem (references 1 and 2) leads to the simultaneous solution of two equations. The degree of each of these equations in the general case of three degrees of freedom (flexure, torsion, and aileron) is three. If, in addition, the effect of a tab motion or a float is desired, the degree of the equations may be more than three. The numerical calculations involving the plotting of roots becomes laborious and time-consuming. A method of elimination for obtaining common roots of two simultaneous equations may be used, which does away with the necessity for any root extractions. (See, for example, reference 3.) The procedure results in the saving of considerable effort, particularly when more than two degrees of freedom are involved. The Sylvester method of obtaining the condition that two simultaneous equations have a common root completely eliminates the unknown quantity. It is feasible, however, to terminate the process of elimination with two equations of the first or second degree. The choice made in the following sections is the use of two equations of the first degree.

The equations arising in the calculations in the case of three degrees of freedom are of the form:

$$\left.\begin{aligned} A_3X^3+A_2X^2+A_1X+A_0=0 \\ B_3X^3+B_2X^2+B_1X+B_0=0 \end{aligned}\right\} \tag{1}$$

where in special cases the degrees of the equations [(3,3) in equation (1)] may be (3,2), (2,2), (2,1), or (1,1). The quantity X is an unknown frequency parameter, and the coefficients A and B are functions of a large number of parameters: structural parameters a, b, c, x_α, x_β, r_α^2, r_β^2, κ, g_α, g_β, and g_h; frequency parameters Ω_h, Ω_α, Ω_β; and the reduced frequency $1/k$. For a particular aircraft structure represented by given parameters there corresponds a flutter velocity and a frequency determined from X and $1/k$. Expressions for the quantities A and B are listed in references 1 and 2. In the following discussion it is assumed that these quantities are available.

The common solution of equations (1) can be obtained from the common solution of

$$\left.\begin{aligned} a_1X+a_0=0 \\ b_1X+b_0=0 \end{aligned}\right\} \tag{2}$$

where a_1, a_0, b_1, and b_0 are functions, listed later, of the A's and B's in equations (1). Now, from equations (2) it is evident that the common solution exists if and only if

$$X_1=-a_0/a_1 \text{ is also equal to } X_2=-b_0/b_1$$

Then, if all the parameters but one are kept constant, for instance $1/k$, and X_1 and X_2 are plotted against $1/k$, the intersection (or intersections) determines the common root (or roots) X and the value (or values) of $1/k$ for which this common solution occurs, and X and $1/k$ together determine the flutter solution for the particular structure.

Another possibility, namely, keeping $1/k$ fixed and plotting X against one of the structural or frequency parameters, will yield as a flutter solution the necessary structural parameter. Many variations are possible.

The Sylvester resultant of equations (2) is the determinant $\begin{vmatrix} a_1 & a_0 \\ b_1 & b_0 \end{vmatrix}$ and its vanishing is the condition for the existence of a common root. If this quantity is plotted against $1/k$ as the abscissa, for instance, the intersection with the $1/k$ axis gives the required value of $1/k$. The first-mentioned method involving two parameters is preferable, however, because the two curves are simpler and yield both X and $1/k$ simultaneously.

There remains, then, only the task of listing the expressions for a_1, a_0, b_1, and b_0. It is convenient to list these expressions separately for the cases in which the degree of the equation is (2, 2), (3, 2), and (3, 3).

In order to obtain a_0, a_1, b_0, and b_1 for the case of two quadratics, multiply the first of equations (1) by B_2 and the second equation by A_2 and subtract; and

similarly multiply the first of equations (1) by B_2X+B_1 and the second by A_2X+A_1 and subtract. Then

$$a_0=\begin{vmatrix} A_0 & A_2 \\ B_0 & B_2 \end{vmatrix}$$

$$a_1=\begin{vmatrix} A_1 & A_2 \\ B_1 & B_2 \end{vmatrix}$$

$$b_0=\begin{vmatrix} A_0 & A_1 \\ B_0 & B_1 \end{vmatrix}$$

$$b_1=\begin{vmatrix} A_0 & A_2 \\ B_0 & B_2 \end{vmatrix}=a_0$$

Similarly, for one cubic and one quadratic (3, 2):

$$a_0=\begin{vmatrix} A_0B_1-A_1B_0 & -B_0A_3 \\ B_0 & B_2 \end{vmatrix}$$

$$a_1=\begin{vmatrix} A_0B_2-A_2B_0 & -B_0A_3 \\ B_1 & B_2 \end{vmatrix}$$

$$b_0=\begin{vmatrix} A_0B_1-A_1B_0 & A_0B_2-A_2B_0 \\ B_0 & B_1 \end{vmatrix}$$

$$b_1=a_0$$

In the case of two cubics

$$a_0=\begin{vmatrix} \begin{vmatrix} A_0 & A_1 \\ B_0 & B_1 \end{vmatrix} & \begin{vmatrix} A_0 & A_3 \\ B_0 & B_3 \end{vmatrix} \\ \begin{vmatrix} A_0 & A_3 \\ B_0 & B_3 \end{vmatrix} & \begin{vmatrix} A_2 & A_3 \\ B_2 & B_3 \end{vmatrix} \end{vmatrix}$$

$$a_1=\begin{vmatrix} \begin{vmatrix} A_0 & A_2 \\ B_0 & B_2 \end{vmatrix} & \begin{vmatrix} A_0 & A_3 \\ B_0 & B_3 \end{vmatrix} \\ \begin{vmatrix} A_1 & A_3 \\ B_1 & B_3 \end{vmatrix} & \begin{vmatrix} A_2 & A_3 \\ B_2 & B_3 \end{vmatrix} \end{vmatrix}$$

$$b_0=\begin{vmatrix} \begin{vmatrix} A_0 & A_1 \\ B_0 & B_1 \end{vmatrix} & \begin{vmatrix} A_0 & A_2 \\ B_0 & B_2 \end{vmatrix} \\ \begin{vmatrix} A_0 & A_3 \\ B_0 & B_3 \end{vmatrix} & \begin{vmatrix} A_1 & A_3 \\ B_1 & B_3 \end{vmatrix} \end{vmatrix}$$

$$b_1=a_0$$

In the use of this method it is sometimes found that the common intersection is not obtained with precision without the use of many values of $1/k$. It may then appear to be more convenient to employ a different form. Thus, in the case of two cubics, there are three possible forms for a_0, a_1, b_0, and b_1 and a second form is

$$a_0=\begin{vmatrix} \begin{vmatrix} A_0 & A_3 \\ B_0 & B_3 \end{vmatrix} & \begin{vmatrix} A_2 & A_3 \\ B_2 & B_3 \end{vmatrix} \\ \begin{vmatrix} A_0 & A_2 \\ B_0 & B_2 \end{vmatrix} & \begin{vmatrix} A_1 & A_3 \\ B_1 & B_3 \end{vmatrix} \end{vmatrix}$$

$$a_1=\begin{vmatrix} \begin{vmatrix} A_1 & A_3 \\ B_1 & B_3 \end{vmatrix} & \begin{vmatrix} A_2 & A_3 \\ B_2 & B_3 \end{vmatrix} \\ \begin{vmatrix} A_0 & A_3 \\ B_0 & B_3 \end{vmatrix}+\begin{vmatrix} A_1 & A_2 \\ B_1 & B_2 \end{vmatrix}, & \begin{vmatrix} A_1 & A_3 \\ B_1 & B_3 \end{vmatrix} \end{vmatrix}$$

$$b_0=\begin{vmatrix} \begin{vmatrix} A_0 & A_3 \\ B_0 & B_3 \end{vmatrix} & \begin{vmatrix} A_1 & A_3 \\ B_1 & B_3 \end{vmatrix} \\ \begin{vmatrix} A_0 & A_2 \\ B_0 & B_2 \end{vmatrix}, & \begin{vmatrix} A_0 & A_3 \\ B_0 & B_3 \end{vmatrix}+\begin{vmatrix} A_1 & A_2 \\ B_1 & B_2 \end{vmatrix} \end{vmatrix}$$

$$b_1=a_0$$

The method is not limited to the original form of the equations. Assume, for example, that *both* X and $1/k$ are preassigned and that it is required to know the values of two parameters, say u_1 and u_2, which have as the flutter solution the preassigned values of X and $1/k$. The original equations can be considered as equations in u_1 and u_2 whose common solution is determined by

$$a_1u_1+a_0=0$$
$$b_1u_1+b_0=0$$

where a_1, a_0, b_1, and b_0 are known (calculable) functions of all the other parameters. If the two roots are plotted against u_2, the intersections (if any) will give the required values of u_1 and u_2.

APPENDIX C

EXAMPLE ON FLUTTER OF BIPLANE

Experiments on the vibration frequencies showed the following results (values given in cycles per min):

1. Antisymmetrical torsion of wing-cellule system	1300
2. Symmetrical bending of wing-cellule system	800
3. Symmetrical torsion of wing-cellule system	1300
4. Local wing bending:	
a. Lower wing, with node at or near interplane strut	1300
b. Upper wing, with node at or near interplane strut	1100
5. Aileron against controls	1100
6. Local torsion in aileron	1800
7. Local torsion in flap	1100
8. Engine rocking	830

There are two possible types of ternary flutter:

a. Symmetrical torsion-symmetrical bending-symmetrical aileron motion. The frequencies are 1300, 800, and 1100, respectively.

b. Antisymmetrical torsion-antisymmetrical bending-antisymmetrical aileron motion. The frequencies are 1300, 0, and 0, respectively.

The other parameters were used as follows:

$a=-0.2$ (elastic axis at 40-percent chord); $x_\alpha=0.2$ (center of gravity at 50-percent chord; the actual center of gravity was near 48-percent chord); $r_\alpha^2=1$; $\kappa=0.2$ (this value of the wing-density parameter corresponds not to sea level but to an altitude of approximately 10,000 ft); $2_b=4$ feet 9 inches (reference chord).

With the use of these parameters, there is obtained for the torsion-bending (case 1) flutter-speed coefficient $v/b\omega_\alpha$ from figure 1 a value of 1.26. The reference velocity $b\omega_\alpha$ is equal to 221 miles per hour. Thus the flutter speed V_F is equal to 278 miles per hour. Because the observed flutter speed on this biplane was lower than this value, (about 200 mph), the aileron was evidently involved. The parameters relating to the aileron were assumed to be as follows:

Location of the center of gravity, x_β	0.002
Radius of gyration, r_β^2	0.002
Chord location, c	0.6

The aileron was considered a full-span aileron. This assumption is fairly reasonable because the lower wing flap was almost identical with the aileron. These values were used in the results shown in figure 1, which was based on the biplane. The ratio $\omega_\beta/\omega_\alpha=0.833$ gives, for the assumed unbalance $x_\beta=0.002$, a value of the flutter coefficient $v/b\omega_\alpha$ of 0.68 or a speed of 151 miles per hour.

For the antisymmetrical case, if a full-span aileron and zero damping are conservatively considered, there is obtained from figure 37 the value $v/b\omega_\alpha=0.41$. A value of the internal damping g_α of 0.01, however, increases the flutter coefficient to 1.18, which is equal to 261 miles per hour (true speed). Notice that this value is calculated without the benefit of a fractional aileron. If there is used in the symmetrical case a small value of the internal damping g_α of 0.01, it is seen from figure 2 (b) that there is only a slight favorable effect from mass-balancing. The flutter coefficient $v/b\omega_\alpha$ is equal to 1.10 for $x_\beta=0.002$ and increases to 1.16 for $x_\beta=-0.002$. With the use of $v/b\omega_\alpha=1.1$, there is obtained a flutter speed of 243 miles per hour (true speed). From later experiments it has been found that the value $g_\alpha=0.01$ is evidently a safe value to use in such calculations. It is thus noted that the flutter speed, because of this effect, approaches the torsion-bending value. It is further observed that with this amount or a larger amount of damping the mass-balancing of the aileron becomes fairly ineffective.

Since the calculation for the symmetrical case based on $g_\alpha=0.01$ gives values of the flutter velocity in the order of 240 miles per hour, true speed (corresponding to an indicated speed of approximately 206 mph), it is probable that this case describes the observed flutter, which was known to be symmetrical.

This biplane was aerodynamically cleaner than many of the earlier types and it is possible that the absence of numerous interplane wires and struts contributed to a lowering of the torsional damping effect to such an extent that flutter was invited. No doubt, many of the older types of biplane were safe from flutter because of their large structural damping.

REFERENCES

1. Theodorsen, Theodore, and Garrick, I. E.: Mechanism of Flutter—A Theoretical and Experimental Investigation of the Flutter Problem. Rep. No. 685, NACA, 1940.
2. Theodorsen, Theodore: General Theory of Aerodynamic Instability and the Mechanism of Flutter. Rep. No. 496, NACA, 1935.
3. Dickson, Leonard Eugene: First Course in the Theory of Equations. John Wiley & Sons, Inc., 1922, ch. X.

TABLE I

[r_α^2, 1; κ, 0.2; c, 0.6; a, −0.2; x_α, 0.2; r_β^2, 0.002; ξ, 1.0]

Figure	$\omega_\beta/\omega_\alpha$	ω_h/ω_α	x_β	g_α	g_β	g_h
1	Variable	0.607	−0.006	0	0	0
	do	.607	−.005	0	0	0
	do	.607	−.002	0	0	0
	do	.607	.002	0	0	0
2 (a)	do	.607	.004	0	0	0
	do	.607	.004	0	0	0
2 (b)	do	.607	.004	.01	0	0
	do	.607	.002	0	0	0
2 (c)	do	.607	.002	.01	0	0
	do	.607	−.002	0	0	0
3	0.833	.607	−.002	.01	0	0
			.002	Variable		

TABLE II

[r_α^2, 1; κ, 0.2; c, 0.6; a, −0.2; r_β^2, 0.002; ξ, 1.0]

Figure	$\omega_\beta/\omega_\alpha$	ω_h/ω_α	x_β	x_α	g_α
4	Variable	0.607	−0.002	0	0
	do	.607	0	0	0
	do	.607	.002	0	0
5 (a)	do	.607	0	0	0
	do	.607	0	0	.01
5 (b)	do	.607	−.002	0	0
	do	.607	−.002	0	.01
	do	.607	.002	.2	0
	do	.607	.002	.2	.01
6	do	.607	.002	0	0
	do	.607	.002	0	.01
	do	.607	.002	−.1	0
7	do	.607	.002	−.1	.01
	do	.607	−.005	−.1	0
	do	.607	−.005	−.1	.01

TABLE III

[r_α^2, 1; κ, 0.2; c, 0.6; a, −0.2; x_β, 0.002; r_β^2, 0.002]

Figure	$\omega_\beta/\omega_\alpha$	ω_h/ω_α	x_α	ξ	g_α
8	Variable	0.607	0.2	0.5	0
	do	.607	.2	.8	0
	do	.607	.2	.9	0
	do	.607	.2	1.0	0
9	0.833	.607	.2	Variable	0
10	Variable	.607	.2	.8	.01
	do	.607	.2	1.0	.01
	do	.607	.2	.8	0
	do	.607	.2	1.0	0
11	do	.607	0	.8	0
	do	.607	0	1.0	.01
	do	.607	0	1.0	0

TABLE IV

[r_α^2, 0.5; κ, 0.2; c, 0.6; a, −0.2; x_α, 0.2; r_β^2, 0.002; ξ, 1.0]

Figure	$\omega_\beta/\omega_\alpha$	ω_h/ω_α	x_β	g_α	g_β	g_h
12	Variable	0.607	−0.005	0	0	0
	do	.607	−.002	0	0	0
	do	.607	0	0	0	0
	do	.607	.002	0	0	0
13 (a)	do	.607	.002	0	0	0
	do	.607	.002	.01	0	0
13 (b)	do	.607	0	0	0	0
	do	.607	0	.01	0	0
13 (c)	do	.607	−.002	0	0	0
	do	.607	−.002	.01	0	0
13 (d)	do	.607	−.005	0	0	0
	do	.607	−.005	.01	0	0
14 (a)	0.607	.607	.002	Variable	Variable	Variable
14 (b)	.833	.607	.002	Variable	Variable	Variable
15 (a)	Variable	.316	.002	0	0	0
	do	.316	.002	.03	0	0
15 (b)	do	1.0	.002	0	0	0
	do	1.0	.002	.03	0	0
15 (c)	do	.316	−.002	0	0	0
	do	.316	−.002	.03	0	0
15 (d)	do	1.0	−.002	0	0	0
	do	1.0	−.002	.03	0	0

TABLE V

[r_α^2, 0.5; c, 0.6; a, −0.2; r_β^2, 0.002; ξ, 1.0]

Figure	$\omega_\beta/\omega_\alpha$	ω_h/ω_α	κ	x_β	x_α	g_α
16	Variable	0.607	0.25	0.002	0.2	0
	do	.607	.25	.002	.2	.01
17	do	.607	.25	.002	0	0
	do	.607	.25	.002	0	.01
18	0.5	Variable	.25	.002	0	0
19	1	do	.25	.002	0	0
	0	do	.2	.002	.2	0
20	0	do	.2	0	.2	0
	0	do	.2	−.002	.2	0
	0	do	.2	−.005	.2	0
21	Variable	.607	.125	.002	.2	0
	do	.607	.125	.002	.2	.01
22	do	.607	.125	−.002	.2	0
	do	.607	.125	−.002	.2	.01
23 (a)	do	.316	.125	.002	.2	0
	do	.316	.125	.002	.2	.03
23 (b)	do	1.0	.125	.002	.2	0
	do	1.0	.125	.002	.2	.03
23 (c)	do	.316	.125	−.002	.2	0
	do	.316	.125	−.002	.2	.03
23 (d)	do	1.0	.125	−.002	.2	0
	do	1.0	.125	−.002	.2	.03
24	0.316	.607	.125	.002	.2	Variable
25	Variable	.607	.083	.002	.2	0
	do	.607	.083	.002	.2	.01
26 (a)	do	.316	.083	0	.2	0
	do	.316	.083	0	.2	.02
26 (b)	do	.607	.083	0	.2	0
	do	.607	.083	0	.2	.02
26 (c)	do	1.0	.083	0	.2	0
	do	1.0	.083	0	.2	.02
27 (a)	do	.316	.083	0	0	0
	do	.316	.083	0	0	.02
27 (b)	do	.607	.083	0	0	0
	do	.607	.083	0	0	.02
27 (c)	do	1.0	.083	0	0	0
	do	1.0	.083	0	0	.02
	do	1.0	.083	0	0	.10
28	do	1.0	.25	.002	0	0

TABLE VI

[r_α^2, 0.25; c, 0.6; a, −0.2; x_α, 0.2; r_β^2, 0.002]

Figure	$\omega_\beta/\omega_\alpha$	ω_h/ω_α	κ	x_β	ξ	g_α
29	Variable	0.607	0.2	0.002	1.0	0
	do	.607	.2	−.002	1.0	0
30 (a)	do	.607	.2	.002	1.0	0
	do	.607	.2	.002	1.0	.01
30 (b)	do	.607	.2	−.002	1.0	0
	do	.607	.2	−.002	1.0	.01
31	do	.607	.2	.002	1.0	0
	do	.607	.2	.002	.8	0
32 (a)	do	.316	.2	.002	1.0	0
	do	.316	.2	.002	1.0	.03
32 (b)	do	1.0	.2	.002	1.0	0
	do	1.0	.2	.002	1.0	.03
32 (c)	do	.316	.2	−.002	1.0	0
	do	.316	.2	−.002	1.0	.03
32 (d)	do	1.0	.2	−.002	1.0	0
	do	1.0	.2	−.002	1.0	.03
33 (a)	do	.316	.125	.002	1.0	0
	do	.316	.125	.002	1.0	.03
33 (b)	do	.607	.125	.002	1.0	0
	do	.607	.125	.002	1.0	.02
33 (c)	do	1.0	.125	.002	1.0	0
	do	1.0	.125	.002	1.0	.05
	do	1.0	.125	.002	1.0	.03
34 (a)	do	.316	.125	−.002	1.0	0
	do	.316	.125	−.002	1.0	.03
34 (b)	do	.607	.125	−.002	1.0	0
	do	.607	.125	−.002	1.0	.01
34 (c)	do	1.0	.125	−.002	1.0	0
	do	1.0	.125	−.002	1.0	.03

TABLE VII

[r_α^2, 0.25; κ, 0.0752; c, 0.5; a, − 0.4; x_α, 0.2; x_β, 0; r_β^2, 0.002]

Figure	$\omega_\beta/\omega_\alpha$	ω_h/ω_α	g_α
35 (a)	Variable	0.316	0
	do	.316	.03
35 (b)	do	.500	0
	do	.500	.03
35 (c)	do	.707	0
	do	.707	.03
35 (d)	do	1.0	0
	do	1.0	.03

TABLE VIII

[r_α^2, 0.25; c, 0.6; a, − 0.4; x_α, 0.2; x_β, 0; r_β^2, 0.0012]

Figure	$\omega_\beta/\omega_\alpha$	ω_h/ω_α	κ	g_α	g_β	g_h
36 (a)	Variable	0.25	0.25	0	0	0
	do	.25	.25	.10	.10	.10
36 (b)	do	.25	.1	0	0	0
	do	.25	.1	.02	.02	.02
	do	.25	.1	.10	.10	.10

TABLE IX

[$\omega_\beta/\omega_\alpha$, 0; ω_h/ω_α, 0; κ, 0.2; c, 0.6; a, − 0.2; x_α, 0.2; r_β^2, 0.002]

Figure	r_α^2	x_β	ξ	g_α
37	1	0.004	1.0	Variable.
	1	.002	1.0	Do.
	1	−.002	1.0	Do.
	1	−.006	1.0	Do.
38	1	.004	Variable	0
	1	.002	do	0
	1	−.002	do	0
	1	−.006	do	0
39	1	Variable	.5	0
	1	do	.6	0
	1	do	.7	0
	1	do	.8	0
	1	do	.85	0
	1	do	.9	0
	1	do	1.0	0
40	.5	.002	1.0	Variable
	.5	−0.002	1.0	Do.
	1	.002	1.0	Do.
	1	−0.002	1.0	Do.
	.25	.002	1.0	Do.
	.25	−.002	1.0	Do.

U. S. GOVERNMENT PRINTING OFFICE: 1943